

3D Printing of Hierarchical Porous Silica and α -Quartz

Florian Putz, Sebastian Scherer, Michael Ober, Roland Morak, Oskar Paris, and Nicola Hüsing*

The ability to macroscopically shape highly porous oxide materials while concomitantly tailoring the porous network structure as desired by simple and environmentally friendly processes is of great importance in many fields. Here, a purely aqueous printing process toward deliberately shaped, hierarchically organized amorphous silica and the corresponding polycrystalline quartz analogues based on a direct ink writing process (DIW) is presented. The key to success is the careful development of the sol–gel ink, which is based on an acidic aqueous sol of a glycolated silane and structure-directing agents. The resulting 3D (DIW) printed silica consists of a macroporous network of struts comprising hexagonally arranged mesopores on a 2D hexagonal lattice. Together with a printed porous superstructure on the millimeter scale, well-defined pore sizes and shapes on at least three hierarchy levels can thus be fabricated. The introduction of devitrifying agents in the printed green part and subsequent heat treatment allows for the transformation of the silica structure into polycrystalline α -quartz. While small pores (micro- and mesopores below 10 nm) are lost, the printed morphology and the macroporous network of struts is preserved during crystallization.

structures on the nanometer scale.^[4,5] The permanently growing 3D printing community has also put effort in the deliberate processing of SiO₂ and researchers have already achieved some breakthroughs such as the preparation of printable silica inks,^[6,7] or the 3D printing of ceramic components like porous scaffolds,^[8–14] and very recently transparent glass.^[15–17] However, there is still a long way to go in the extension of design possibilities, solvent-free processing, etc., and therefore in the exploration of novel synthesis routes.

3D printing of hierarchically organized silica structures with multilevel porosity and well-defined pore sizes and shapes is a challenging task that has to the best of our knowledge not been achieved so far. A bottom-up route toward monolithic materials exhibiting such characteristics is sol–gel processing of condensable silanes in the presence of porogens and phase-separation inducing agents.^[18–20] While silica


SiO₂ in all its forms and phases belongs to the most abundant materials on our planet. It is used in a large variety of applications due to its exceptional properties, e.g., high transparency of fused silica glass in the visible light region, excellent thermal insulating properties of porous silica gels, or a large piezoelectric effect in quartz, to name just a few.^[1–3] The need to deliberately fabricate and design silica-based materials has been evident for decades and gained further interest in recent years with the emergence of approaches to create tailor-made

sols or block copolymers (as an example of a typical porogen) can individually be processed with different printing techniques,^[8,21] a combined sol–gel ink experiencing phase separation is considerably more difficult to print due to disparate flow characteristics of the constituting phases.

Another promising technique with high potential to supplement 3D printing of silica is the crystallization of amorphous structures at small length scales. This has gained increasing interest in recent years mainly due to the development of new, low temperature routes for the devitrification of amorphous silica to yield α -quartz without complete loss of structural features. In 2011, Brinker and co-workers presented a method for the hydrothermal synthesis of α -quartz nanospheres using Stöber silica colloids as amorphous precursors and NaCl as well as alkali hydroxide as mineralizers.^[22] In another approach, Drisko et al. demonstrated the preparation of hollow α -quartz spheres by the crystallization of corresponding amorphous structures between 800 and 1000 °C in the presence of alkaline earth metal ions.^[23] Feature sizes of around 80 nm could be well preserved by this method, but mesoporosity was lost during crystallization. Similar routes have also been used for the devitrification of nanoporous silica films.^[24] Transformation of complex shaped biogenic silica to a mixture of crystalline phases, containing cristobalite and others was shown by Sapei et al.^[25] Despite these ongoing research efforts, the crystallization of hierarchical, man-made silica monoliths has not been demonstrated so far.

F. Putz, S. Scherer, M. Ober, Prof. N. Hüsing
Chemistry and Physics of Materials
Paris Lodron University Salzburg
5020 Salzburg, Austria
E-mail: nicola.huesing@sbg.ac.at

Dr. R. Morak, Prof. O. Paris
Institute of Physics
Montanuniversitaet Leoben
8700 Leoben, Austria

 The ORCID identification number(s) for the author(s) of this article can be found under <https://doi.org/10.1002/admt.201800060>.

© 2018 The Authors. Published by WILEY-VCH Verlag GmbH & Co. KGaA, Weinheim. This is an open access article under the terms of the Creative Commons Attribution License, which permits use, distribution and reproduction in any medium, provided the original work is properly cited.

DOI: 10.1002/admt.201800060

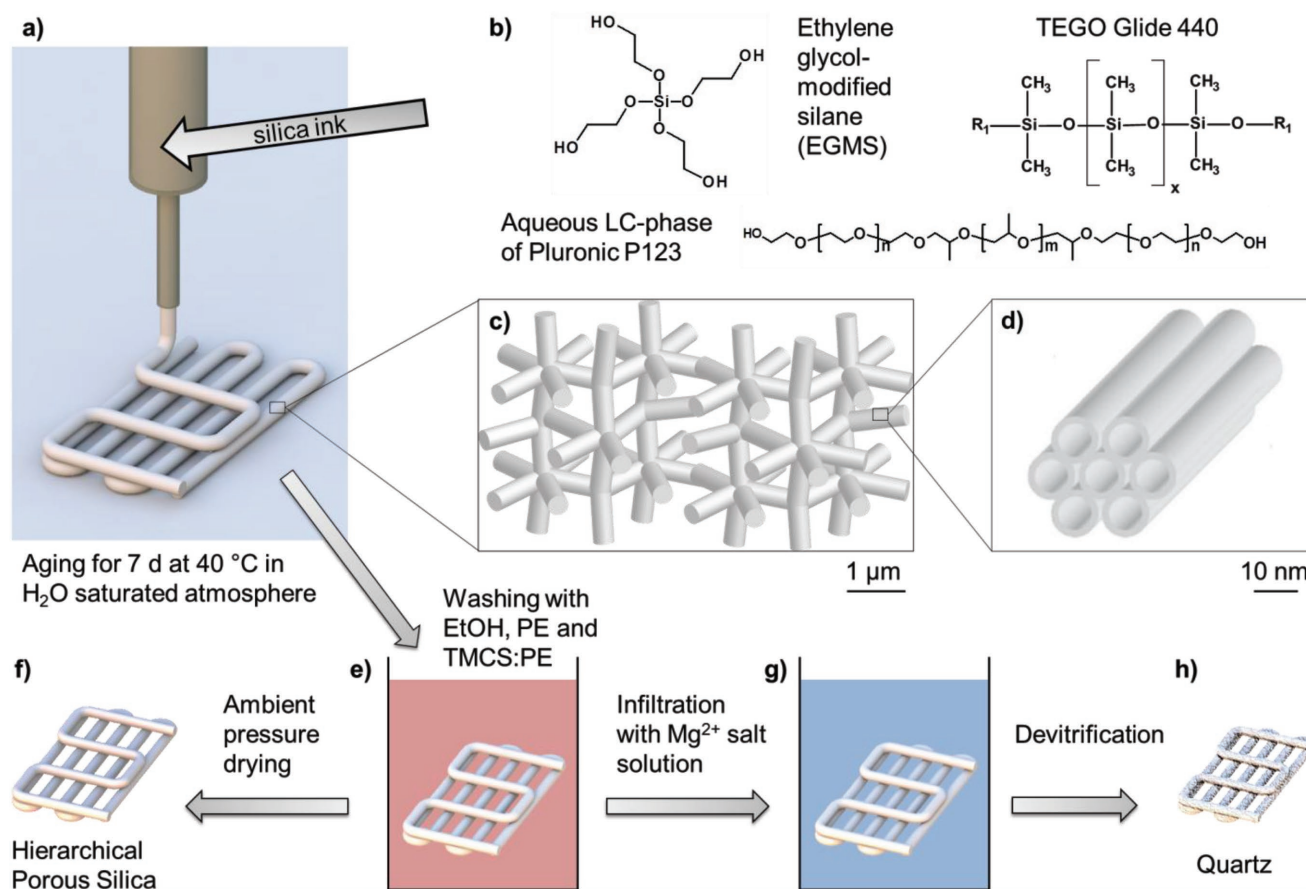


Figure 1. Schematic illustration of the synthesis route towards 3D printed hierarchically structured silica and α -quartz. a) The printable silica ink is extruded in a direct writing approach. b–d) A finely balanced composition of precursors enables the formation of a macroporous network of struts comprising hexagonally arranged mesopores. e) The fabricated objects are aged at 40 °C for 7 d in water vapor saturated atmosphere and then subjected to surfactant extraction and surface silylation via a treatment with ethanol (EtOH), petroleum ether (PE), and a mixture of PE and chlorotrimethylsilane, respectively. f) While ambient pressure drying of these gels leads to hierarchical porous silica, g) infiltration of the network with an aqueous solution of Mg²⁺-ions, and h) subsequent devitrification allows for the transformation of the macroporous cellular structure into polycrystalline α -quartz.

Here we extend the current state-of-the-art of printing processes toward silica significantly by 1) creating an organic solvent-free sol–gel ink that enables 3D printing of hierarchical silica structures with multilevel porosity and 2) crystallizing these printed objects upon retaining their shape and morphological features. We present a manufacturing process covering these aspects for the first time in 3D SiO₂ printing. At first, the synthesis route leads to hierarchical porous silica with defined pore structures on at least three hierarchical levels. Based on this approach, a slight modification of the synthesis protocol enables the transformation of printed structures into polycrystalline, porous α -quartz.

The fabrication of the materials starts with the preparation of a printable silica ink derived from a synthesis described recently by Putz et al.^[26] This one-pot approach, using an ethylene glycol modified silane (EGMS), tetrakis(2-hydroxyethyl) orthosilicate, in combination with an aqueous liquid crystal phase of the surfactant Pluronic P123, which is an amphiphilic polyethylene oxide-polypropylene oxide based triblock copolymer, to create hierarchical porous silica, was modified by the addition of the block copolymer TEGO Glide 440 (Evonik) containing a central polydimethylsiloxane (PDMS) block

(Figure 1b). This rheological additive enables the adjustment of flow characteristics (e.g., homogeneous material flow) during the printing process and allows for the prevention of cracks or rough surfaces in the final structure. However, it strongly influences the structure formation as seen for the macroporous network if the added amount is too high (details are given in Figures S1 and S2 in the Supporting Information). 0.8 wt% TEGO Glide 440 of the precursor composition was found to conveniently combine improved rheological behavior of the sol–gel ink and desired structural properties of the final printed object. The thus prepared sol was kept at 40 °C for several hours, promoting condensation reactions and as a result increasing the sol viscosity and inducing gelation, which is a prerequisite for shape retention and gap spanning features in the printed geometries. It should be noted that there is no need for a binder in the silica ink preparation.

For the creation of hierarchical porous silica with multilevel porosity, direct ink writing (DIW) of the preformed gel was applied (see scheme in Figure 1a). In a series of preliminary tests, all relevant printing parameters, such as printing speed, extrusion rate, the amount of additive, and the reaction time before printing, were adjusted in a way to achieve an appropriate

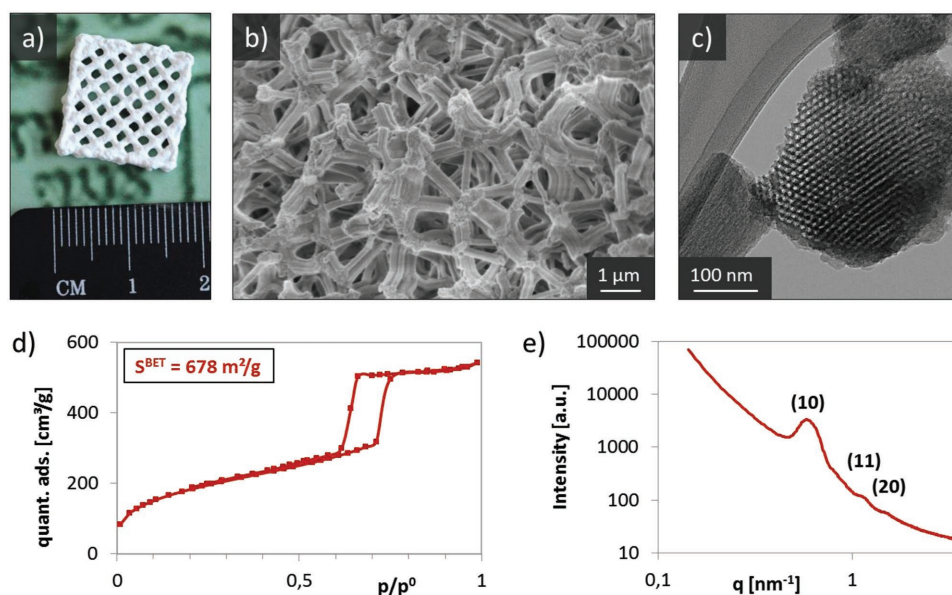


Figure 2. 3D printed hierarchical porous silica. a) The printed 5-layer scaffold structure (optical photograph) consists of b) a macroporous network of struts (SEM image) comprising c) well-ordered, cylindrical mesopores (TEM image). d) Nitrogen sorption analysis confirms a high specific surface area of the silica network and a 2D hexagonal arrangement of the accessible mesopores can be deduced from the corresponding e) SAXS pattern. The numbers in panel (e) denote the Miller indices of the Bragg reflections.

print image. Especially the right timing regarding the progressing condensation reactions is a crucial parameter and was found to be best after five to six hours at 40 °C, even after gelation and phase separation of the gel.^[26] In this state, no fluidity of the gel can be observed when the container is turned (see Figure S3 in the Supporting Information). DIW is possible, because at this stage in the gel formation process still a large number of unreacted monomers or oligomers are available, allowing for further condensation reactions even after remodeling of the gel body. In addition, DIW of this aqueous sol does not require any special conditions like a certain atmosphere or a protective environment directly after printing. Typical problems, such as rapid drying of the samples due to evaporation of the solvent, can be excluded. The printable ink consists of a weakly connected silica network of struts that can be reshaped during direct writing. All strut-like features are transferred to the printed “green body” (Figure 1c), which is composed of a network of struts with each strut containing hexagonally arranged block copolymer/silica hybrid structures aligned along the cylinder axis (Figure 1d). Together with the printed shape and the macroporous network of struts, these anisotropic mesopores form three geometrically well-defined hierarchy levels. This offers a huge playground for advanced characterization methods^[27] or even for mechanical modeling,^[28] but also for a number of applications, including separation, sensing and actuation,^[20] or bioinspired materials design,^[29,30] to name just a few.

After printing, the green part was transferred into a water vapor saturated chamber and kept at 40 °C for 7 d to facilitate coalescence/healing of the partially disconnected strut network through condensation of remaining hydrolyzed precursor molecules as well as by Ostwald ripening. The aged gel was subjected to an extraction procedure with ethanol (EtOH) and petroleum ether (PE), followed by a surface functionalization

with chloro(trimethyl)silane (TMCS) to enable subsequent drying at ambient pressure (Figure 1e,f).

The resulting dried hierarchically organized porous silica object is characterized by a simple printed scaffold structure with five layers and a mesh thickness of about 0.8 mm as shown in Figure 2a. Without further heat treatment the printed silica structure still contains alkoxy moieties, adsorbed water and/or alcohol, and due to the silylated surface a significant amount of organic groups on the surface. Thermogravimetric analysis (TGA) measurements (not shown) confirm about 30 wt% of organic residue in the material. Structural investigations by scanning electron microscopy (SEM), transmission electron microscopy (TEM), and small-angle X-ray scattering (SAXS) confirm the existence of a macroporous network of struts (Figure 2b) exhibiting cylindrical mesopores on a 2D hexagonal lattice (Figure 2c) with a repeating unit distance of 11 nm (determined from the SAXS pattern in Figure 2e). Typical specific surface areas are in the range of 650–700 m² g⁻¹ as calculated from nitrogen adsorption analysis (exemplary isotherm shown in Figure 2d) using the Brunauer–Emmett–Teller (BET) method.

For the fabrication of 3D printed α -quartz, the above described synthesis protocol was modified after the solvent extraction procedure. The wet alcogels were infiltrated with a 0.1 M aqueous solution of MgCl₂ (Figure 1g), providing Mg²⁺ ions that act as devitrifying agent in the subsequent crystallization step. A uniform distribution of these ions is facilitated by the large number of mesopores ($V_{\text{meso}} = 0.75\text{--}0.80\text{ cm}^3\text{ g}^{-1}$) and also micropores ($V_{\text{micro}} = 0.02\text{--}0.03\text{ cm}^3\text{ g}^{-1}$) within the hierarchical silica network, enabling a homogeneous devitrification. Furthermore, the applied surface silylation allows for simple evaporative drying before crystallization without collapse of the silica network. Tedious drying methods like supercritical drying with the risk of washing out Mg²⁺ ions can thus be

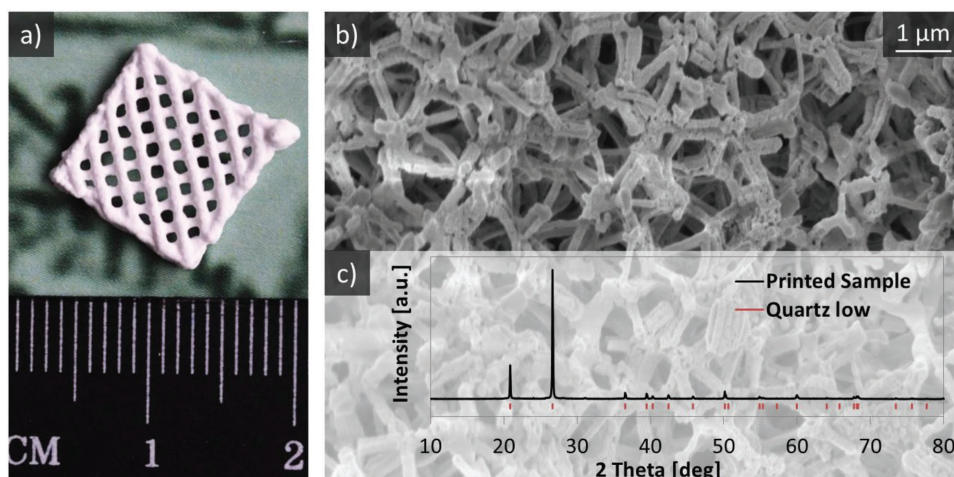


Figure 3. 3D printed polycrystalline α -quartz. The macroscopic shape of the printed object (a) optical photograph) and the morphology of the macro-porous network of struts (b) SEM image) remain (except for shrinkage) almost unchanged after crystallization. c) The successful transformation into α -quartz (quartz low) can be confirmed by XRD.

avoided. Through this approach, the crystallization of silica can be conducted at relatively low temperatures of around 1100 °C, allowing for the conservation of morphological features as small as 10 nm and avoiding strong sintering effects.^[19] The final temperature program was adjusted in a way that provided pure α -quartz (Figure 1h; more details in Figure S4 in the Supporting Information).

A scaffold with similar shape and the same original dimensions as shown for hierarchical silica was used to demonstrate the impact of crystallization. The macroscopic shape remains unaffected (Figure 3a), but a linear shrinkage of about 30% occurs (compare Figure S5 in the Supporting Information), enabling a further reduction in achievable geometric feature sizes. Moreover, the macroscopic strut network survives crystallization (see SEM image in Figure 3b) with only minor changes in morphology, e.g., a slight coarsening of the struts. However, smaller pores like meso- and micropores are destroyed during the devitrification due to crystal growth and sintering effects which can be confirmed by TEM investigations (Figure S6, Supporting Information) as well as results from nitrogen adsorption analysis with specific surface areas below 20 m² g⁻¹. The (linear) shrinkage of about 30% can be related to several factors, one being the decomposition of residual organic groups and loss of mesoporosity concomitant with loss in specific surface area due to sintering effects, but also to the increase in density from amorphous silica (2.2 g cm⁻³) to crystalline quartz (2.65 g cm⁻³). Accordingly, the bulk density increases from 0.2–0.3 g cm⁻¹ before crystallization to 0.6–0.8 g cm⁻¹ after crystallization as shown for monolithic samples (Figure S5, Supporting Information). The successful crystallization of the printed structure can be proven by X-ray diffraction (XRD), indicating phase pure α -quartz (Figure 3c; Figure S4, Supporting Information).

In summary, deliberately shaped, hierarchically organized porous silica has been fabricated by direct ink writing 3D printing for the first time. The development of an aqueous-based sol-gel ink allows for solvent free processing, thus not only dispensing the need for organic solvents, but also

facilitating the 3D printing process because solvent evaporation is omitted. The printed green bodies can easily be dried at ambient conditions after extraction of the structure-directing agent as well as the rheological additive. In a second approach, the printed green body can be infiltrated with devitrifying agents, such as alkaline earth metal ions, thus facilitating crystallization to yield α -quartz. Cellular macroporosity and shape of the green body are retained upon crystallization, while all features show a linear shrinkage of about 30%. Both routes demonstrate the high potential of 3D printing aided materials design for porous SiO₂ by presenting a fabrication technique beyond state of the art and by providing access to extraordinary structural features. The sol-gel process can be readily tuned for the preparation of a wide variety of different compositions, including other metal oxides, but also hybrid systems. In addition, the recently demonstrated procedure for creating anisotropic pore structures by shear-induced alignment via extrusion of a preformed gel could pave the way for the application of such materials as sorption-driven actuators or even in the field of nanofluidics.^[26] With that, the DIW technology has seen a major progress, now allowing for the fabrication of very unique structures that are not accessible via conventional processing methods.

Experimental Section

Synthesis of a Printable Silica Ink and 3D Printing, Aging, and Washing of Porous Silica: The synthesis of the silica ink was performed using tetrakis(2-hydroxyethyl)orthosilicate (EGMS) as the precursor according to Putz et al.^[26] Wet gel preparation was conducted by adding TEGO Glide 440 (Evonik Resource Efficiency GmbH) and EGMS to a homogeneous mixture of 30 wt% P123 (Sigma-Aldrich) in 1 M HCl (aq) with a composition by weight (Si/P123/HCl) of 8.4/30/70. In a series of experiments the amount of TEGO Glide 440 was varied from 0 to 3 wt% of the precursor composition. Stirring for 1 min yielded a clear, viscous liquid that was filled into polypropylene (PP) syringes of 5 mm diameter, and allowed to gel at 40 °C for 5–6 h. The prepared syringes were loaded on a commercial 3D printer of type Engine E3 with a SDS-5 extruder (both Hyrel 3D) and the silica gel was printed at constant displacement

rates through a nozzle diameter of 800 μm , producing a linear feed rate of about 10 mm s^{-1} . Further gelation and aging of the printed structures was performed at 40 $^{\circ}\text{C}$ for 7 d in a water vapor saturated atmosphere. The aged gels were treated with ethanol (EtOH), PE, and a mixture of TMCS and petroleum ether (TMCS:PE = 10:90 by weight) in the order EtOH-PE-TMCS/PE-PE-EtOH for 24 h each. Drying was performed at ambient conditions (25 $^{\circ}\text{C}$) for 7 d.

Crystallization of Porous Silica into Porous α -Quartz: The washed and silylated, wet printed structures were impregnated with an aqueous 0.1 mol L^{-1} MgCl_2 solution for 5 h and then dried at ambient conditions (25 $^{\circ}\text{C}$) for 7 d. Crystallization of the printed silica structures was performed at 1100 $^{\circ}\text{C}$ for 5 h in air with a heating rate of 10 $^{\circ}\text{C min}^{-1}$.

Electron Microscopy: SEM images were taken using a ZEISS FE-SEM ULTRA PLUS applying its in-lens secondary electron detector at an accelerating voltage of 2 kV. The microstructure of the samples was studied by TEM with a TECNAI F20 field emission electron microscope operated at an accelerating voltage of 200 kV. Images were recorded with a Gatan Orius SC600 CCD camera.

Nitrogen Sorption: Nitrogen adsorption-desorption measurements were carried out at 77 K using a Micrometrics ASAP 2420. The specific surface area was calculated with the BET 5-point method in the relative pressure range of 0.05–0.3. Prior to the measurement the samples were degassed in vacuum for 16 h at 110 $^{\circ}\text{C}$.

SAXS: SAXS measurements were performed with a Nanostar laboratory instrument (Bruker AXS, Karlsruhe, Germany) using $\text{CuK}\alpha$ radiation and a Vantec 2000 detector at a sample-detector distance of 711 mm. The beam was monochromatized and focused by a graded multilayer mirror and defined by two scatterless pinholes of 300 μm in diameter. 2D SAXS patterns were corrected for background and transmission and averaged to obtain the intensity $I(q)$ as a function of the scattering vector length q ($q = 4\pi \sin \theta / \lambda$, θ being half the scattering angle and $\lambda = 0.154$ nm the X-ray wavelength). The lattice parameter of the 2D hexagonal mesopore lattice was determined from the position of the first-order Bragg peak by $a = 4\pi / (\sqrt{3} q_{10})$.

XRD: Powder X-ray diffraction (PXRD) measurements ($5^{\circ} \leq 2\theta \leq 180^{\circ}$, continuous scan) were carried out on powdered samples in reflection-mode on a BRUKER D8 DaVinci Design diffractometer using $\text{CuK}\alpha$ radiation, fixed 0.3 $^{\circ}$ divergence slit, 0.04 rad Soller slits, antiscatter slit 4.0 $^{\circ}$, and a Lynxeye detector.

Supporting Information

Supporting Information is available from the Wiley Online Library or from the author.

Acknowledgements

The authors thank Grant Osborne (Paris Lodron University Salzburg) for providing technical assistance with 3D printing. The authors acknowledge financial support from the Austrian Science Foundation FWF (Project I 1605-N20).

Conflict of Interest

The authors declare no conflict of interest.

Keywords

3D printing, crystallization, hierarchical porous silica, sol-gel inks, α -quartz

Received: February 19, 2018

Revised: April 3, 2018

Published online:

- [1] I. Fanderlik, *Silica glass and its Application*, Elsevier, New York, USA **2013**.
- [2] N. Hüsing, U. Schubert, *Angew. Chem., Int. Ed.* **1998**, *37*, 22.
- [3] B. Jaffe, *Piezoelectric Ceramics*, Vol. 3, Elsevier, New York, USA **2012**.
- [4] C. T. Kresge, M. E. Leonowicz, W. J. Roth, J. C. Vartuli, J. S. Beck, *Nature* **1992**, *359*, 710.
- [5] D. Zhao, J. Feng, Q. Huo, N. Melosh, G. H. Fredrickson, B. F. Chmelka, G. D. Stucky, *Science* **1998**, *279*, 548.
- [6] E. B. Duoss, M. Twardowski, J. A. Lewis, *Adv. Mater.* **2007**, *19*, 3485.
- [7] J. E. Smay, J. Cesarano, J. A. Lewis, *Langmuir* **2002**, *18*, 5429.
- [8] J. E. Smay, G. M. Gratson, R. F. Shepherd, J. Cesarano, J. A. Lewis, *Adv. Mater.* **2002**, *14*, 1279.
- [9] J. A. Lewis, *Adv. Funct. Mater.* **2006**, *16*, 2193.
- [10] Q. Fu, E. Saiz, A. P. Tomsia, *Adv. Funct. Mater.* **2011**, *21*, 1058.
- [11] C. Wu, Y. Luo, G. Cuniberti, Y. Xiao, M. Gelinsky, *Acta Biomater.* **2011**, *7*, 2644.
- [12] L. Chen, X. Tang, P. Xie, J. Xu, Z. Chen, Z. Cai, P. He, H. Zhou, D. Zhang, T. Fan, *Chem. Mater.* **2018**, *30*, 799.
- [13] M. A. Torres Arango, D. Kwakye-Ackah, S. Agarwal, R. K. Gupta, K. A. Sierros, *ACS Sustainable Chem. Eng.* **2017**, *5*, 10421.
- [14] C. Minas, D. Carnelli, E. Tervoort, A. R. Studart, *Adv. Mater.* **2016**, *28*, 9993.
- [15] F. Kotz, K. Arnold, W. Bauer, D. Schild, N. Keller, K. Sachsenheimer, T. M. Nargang, C. Richter, D. Helmer, B. E. Rapp, *Nature* **2017**, *544*, 337.
- [16] D. T. Nguyen, C. Meyers, T. D. Yee, N. A. Dudukovic, J. F. Destino, C. Zhu, E. B. Duoss, T. F. Baumann, T. Suratwala, J. E. Smay, R. Dylla-Spears, *Adv. Mater.* **2017**, *29*, 1701181.
- [17] J. F. Destino, N. A. Dudukovic, M. A. Johnson, D. T. Nguyen, T. D. Yee, G. C. Egan, A. M. Sawvel, W. A. Steele, T. F. Baumann, E. B. Duoss, T. Suratwala, R. Dylla-Spears, *Adv. Mater. Technol.* **2018**, <https://doi.org/10.1002/admt.201700323>.
- [18] K. Nakanishi, N. Tanaka, *Acc. Chem. Res.* **2007**, *40*, 863.
- [19] C. Triantafillidis, M. S. Elsaesser, N. Hüsing, *Chem. Soc. Rev.* **2013**, *42*, 3833.
- [20] A. Feinle, M. S. Elsaesser, N. Hüsing, *Chem. Soc. Rev.* **2016**, *45*, 3377.
- [21] M. S. Onses, C. Song, L. Williamson, E. Sutanto, P. M. Ferreira, A. G. Alleyne, P. F. Nealey, H. Ahn, J. A. Rogers, *Nat. Nanotechnol.* **2013**, *8*, 667.
- [22] X. Jiang, Y.-B. Jiang, C. J. Brinker, *Chem. Commun.* **2011**, *47*, 7524.
- [23] G. L. Drisko, A. Carretero-Genevri, A. Perrot, M. Gich, J. Gazquez, J. Rodriguez-Carvajal, L. Favre, D. Grosso, C. Boissiere, C. Sanchez, *Chem. Commun.* **2015**, *51*, 4164.
- [24] G. L. Drisko, A. Carretero-Genevri, M. Gich, J. Gázquez, D. Ferrah, D. Grosso, C. Boissière, J. Rodriguez-Carvajal, C. Sanchez, *Adv. Funct. Mater.* **2014**, *24*, 5493.
- [25] L. Sapei, R. Nöske, P. Strauch, O. Paris, *Chem. Mater.* **2008**, *20*, 2020.
- [26] F. Putz, R. Morak, M. S. Elsaesser, C. Balzer, S. Braxmeier, J. Bernardi, O. Paris, G. Reichenauer, N. Hüsing, *Chem. Mater.* **2017**, *29*, 7969.
- [27] R. Morak, S. Braxmeier, L. Ludescher, F. Putz, S. Busch, N. Hüsing, G. Reichenauer, O. Paris, *J. Appl. Crystallogr.* **2017**, *50*, 1404.
- [28] C. Balzer, A. M. Waag, S. Gehret, G. Reichenauer, F. Putz, N. Hüsing, O. Paris, N. Bernstein, G. Y. Gor, A. V. Neimark, *Langmuir* **2017**, *33*, 5592.
- [29] U. G. K. Wegst, H. Bai, E. Saiz, A. P. Tomsia, R. O. Ritchie, *Nat. Mater.* **2014**, *14*, 23.
- [30] A. Sydney Gladman, E. A. Matsumoto, R. G. Nuzzo, L. Mahadevan, J. A. Lewis, *Nat. Mater.* **2016**, *15*, 413.